Mem. S.A.It. Vol. 76, 523

Memorie della

Numerical high energy radiation modeling of selected millisecond pulsars

Michal Frackowiak[1] and Bronislaw Rudak[1,2]

[1] Copernicus Astronomical Center, Rabianska 8, 87-100 Torun, Poland
[2] Dept. of Astronomy and Astrophysics, NCU, Torun, Poland

Abstract. We present spectral and directional properties of gamma radiation obtained by numerical modeling of selected millisecond pulsars, i.e. PSR J0218+4232, PSR J0437-4715 and PSR B1821-24. The general relativistic space charge limited flow model of Muslimov & Harding (1997) in its version of an unscreened accelerating electric field was used. The results give both general ideas and constraints on the specific character of magnetospheric activity in each of these pulsars. We also draw conclusions for possible observations of these pulsars within the ultrarelativistic energy range above 100 GeV with Cherenkov telescopes such as MAGIC or H.E.S.S.

Key words. millisecond pulsars – gamma-rays – polar-cap emission

1. Introduction

Three millisecond pulsars have been recently drawing quite an attention within the gamma-ray astrophysics community: PSR J0218+4232, PSR B1821-24 and PSR J0437-4715. E.g. Bulik et al. (2000) argued that in the case of polar-cap activity due to a vacuum-gap-like strong electric field, PSR J0437-4715 would be within reach of high-sensitivity Cherenkov telescopes of the future. With fully operating HESS (Konopelko, 1999) and MAGIC (Baixeras, 2003), sensitive above $\sim$ 50 GeV, the questions concerning observability of at least some millisecond pulsars may get answered (Konopelko, 2002).

PSR J0218+4232 with PSR B1821-24, and PSR J0437-4715 represent two apparently distinct classes of millisecond pulsars as far as their X-ray properties are concerned (Kuiper et al., 1998). The first class members are regarded as "mini Crabs", whereas non-thermal activity of PSR J0437-4715 is much weaker, its X-ray emission being dominated by a thermal component. However, little is known about their gamma-ray properties within the EGRET range of energies above 100 MeV.

In this paper we address the issue of polar cap activity in millisecond pulsars as proposed and elaborated by Muslimov & Harding (1997) and Harding & Muslimov (1998).

We present numerical results of modeling PSR J0218+4232, PSR J0437-4715 and PSR B1821-24 using a 3-dimensional relativistic approach and Monte Carlo simulations. Comparison of the results with available observational data and/or constraints leads to conclusions which may shed some light on the specific character of magnetospheric activity in each of these three pulsars.

2. The model

As a framework we use a general relativistic SCLF (space charge limited flow) polar-cap model of Muslimov & Harding (1997) in its version with an unscreened accelerating electric field (denoted hereafter as SCLF-USEF). This version is thought to be relevant for millisecond pulsars (Harding et al., 2002) and takes General Relativity (GR) effects into account. Weak magnetic fields ($\sim 10^8$ to $\sim 10^9$ Gauss) make the magnetic photon absorption relatively inefficient. Contrary to the case of classical pulsars, electron-positron pairs created in magnetic absorption are not capable of forming a well defined pair formation front that would screen out the accelerating field $E_\parallel$. As a consequence $E_\parallel$ which accelerates primary electrons from the polar cap surface to relativistic energies along open magnetic field lines can extend up to a few stellar radii. Its strength varies across the cap; moreover, it depends on the inclination angle of the pulsar.

We used analytical formulae for unscreened $E_\parallel$ as derived by Harding & Muslimov (1998). These were incorporated in our numerical code simulating radiative processes due to electrons subject to acceleration along dipolar magnetic field lines. The code included careful treatment of aberration due to rotation as well as photon-travel-time delays. That allowed us to perform a detailed 3-dimensional analysis of the radiation. The condition of a small number of pair-creation events was fulfilled in all the cases considered, making the model self-consistent.

In the analysis presented below we have neglected inverse Compton scattering. We focused on the main component contributing to the high-energy emission in the range between 100 MeV and few tens of GeV, which is curvature radiation (of primary electrons) dominated.

3. PSR J0218+4232

This is the only millisecond pulsar for which detection has been claimed of pulsed high-energy emission with EGRET (Kuiper et al., 2000). The pulsar parameters used in this work are: spin period $P = 2.323$ ms, inferred magnetic field strength at the polar cap $B_{\rm pc} = 8.58 \cdot 10^8$ Gauss, and distance $d = 5.85$ kpc. The pulsar is probably a nearly aligned rotator (Stairs et al., 1999). Accordingly, the geometrical configuration we have chosen for modeling is: inclination angle (angle between the spin axis and the magnetic axis) $\alpha = 20°$, observer's colatitude (angle between the spin axis and the l.o.s.) $\zeta = 16°$. Fig. 1 presents the results of numerical modeling of the radiation field for PSR J0218+4232. Two EGRET data points along with upper limits from EGRET and COMPTEL (after Kuiper et al., 2000) are overlaid on the phase-averaged model spectrum for comparison.

Clearly, the SCLF-USEF model in its present form is not reproducing satisfactorily either the observed spectrum or the lightcurve for low values of α and ζ. An extra component would be required to fit the two EGRET points in the phase-averaged gamma-ray spectrum. Possible candidates (associated with the pairs) for such a component were proposed by Rudak & Dyks (2002), and recently by Harding et al. (2005). As far as the lightcurve is concerned, the result obtained by Kuiper et al. (2000), even though based on a very small number of counts, shows two asymmetric pulses while the model cannot reproduce this asymmetry.

These apparent problems motivated us to create a toy model with a parameterized electric field $E_\parallel$. We were inspired by an apparently successful caustic slot gap model for young classical pulsars (Dyks & Rudak, 2003; Muslimov & Harding, 2004). Fig. 2 presents the results for a variant of the caustic slot gap model, with an accelerating electric field of constant strength of $\sim 2 \cdot 10^3$ Gauss reaching an altitude of 2 stellar radii above the surface, and extending along the thin outer rim of the polar cap. Rotational effects result in asymmetry of the peaks. At the same time, the relatively low value of $E_\parallel$ allows to obtain the desired spectral slope to fit the two EGRET points and obeying all the upper-limits at the same time.

A possibility that caustic slot gaps might be relevant for other "mini Crabs", very much like caustic slot gaps proposed for the Crab pulsar, deserves theoretical studies.

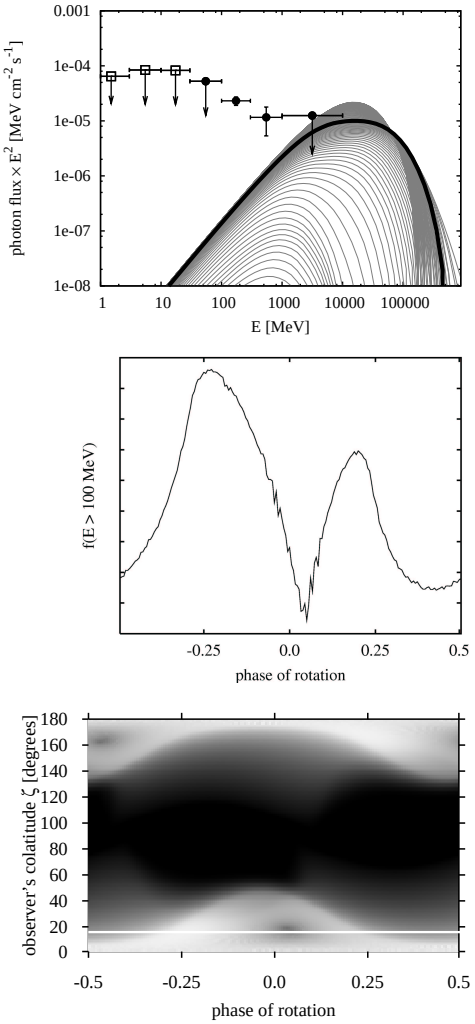

Fig. 1. Results for PSR J0218+4232, inclination angle $\alpha = 20°$. The upper panel shows the phase-averaged spectrum for the preferred choice of viewing angle $\zeta = 16°$ (bold line), with a family of spectra for a range of values of ζ (grey lines). Filled circles correspond to EGRET observations while open squares – to COMPTEL. The middle panel shows the lightcurve corresponding to $\zeta = 16°$ for photons above 100 MeV The bottom panel presents photon mapping in the plane (ζ, phase of rotation) with intensity of white color proportional to the photon flux above 100 MeV. White horizontal line shows the cut of the l.o.s. at $\zeta = 16°$ across the map; this cut yields the lightcurve shown in the middle panel.

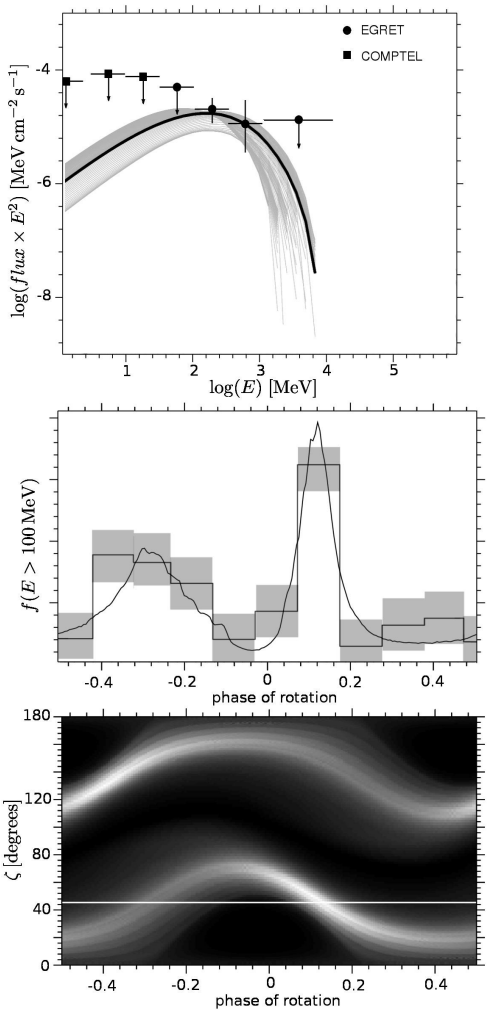

Fig. 2. Results for the "caustic" toy-model model for PSR J0218+4232 with $\alpha = 25°$ and $\zeta = 47°$. See Fig. 1 for the description of panels. In the middle panel the observational data (histogram) from Kuiper et al. (2000) and 1-σ error-boxes is overlaid.

4. PSR J0437-4715

Despite its proximity (140 pc) and very high spin-down flux, this pulsar was not detected by EGRET; an upper-limit for pulsed emission above 100 MeV was set at the level of $2.1 \cdot 10^{-7}$ cm^{-2} s^{-1} (Fierro et al., 1995). This

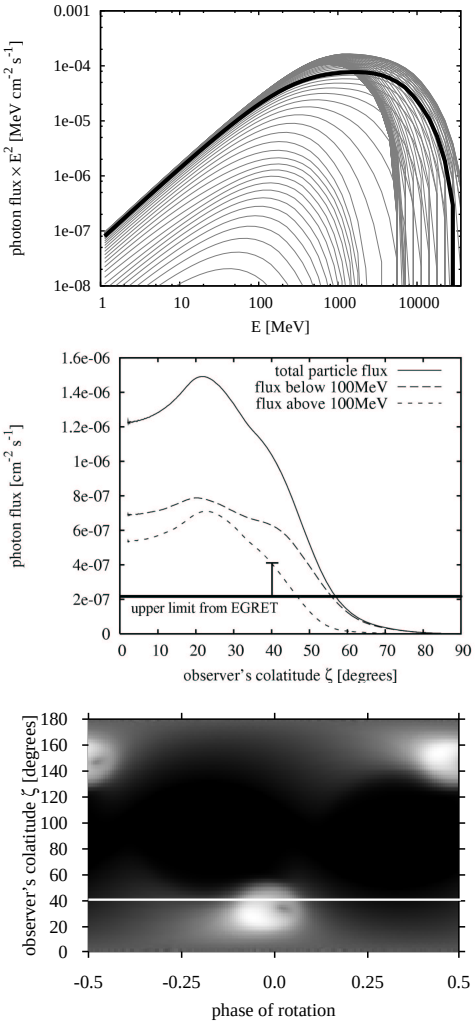

Fig. 3. Results for PSR J0437-4715 with $\alpha = 35°$ and $\zeta = 40°$. For top and bottom panel description see Fig. 1. The middle panel represents expected photon flux ($E_{\rm ph} > 100$ MeV) for fixed $\alpha = 35°$ and varying ζ along with the EGRET upper limit for emission above 100 MeV.

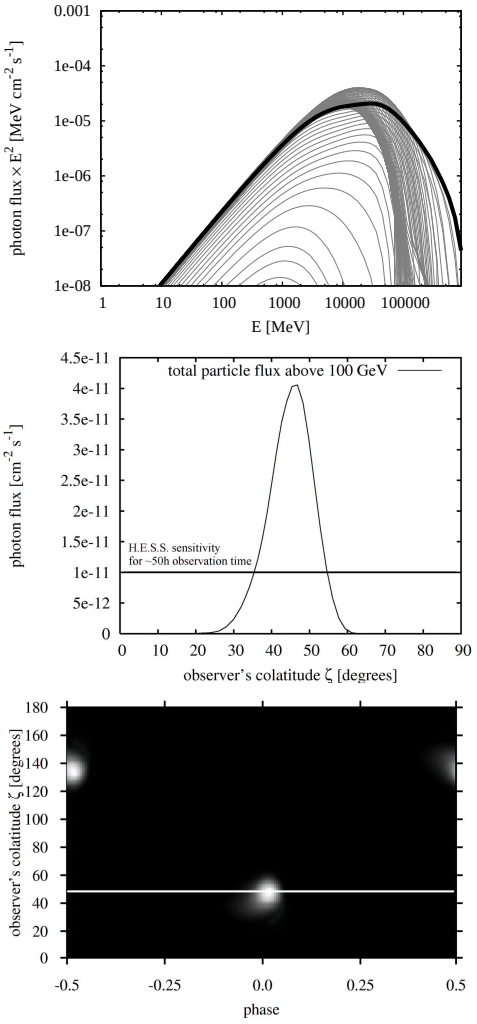

Fig. 4. Results for PSR B1821-24, $\alpha = 50°$. The upper panel shows the family of spectra as seen with different ζ with the "most energetic" spectrum for $\zeta = 48°$ shown in bold. The middle panel presents expected photon flux $E_{\rm ph} > 100$ GeV for fixed $\alpha = 50°$ and varying ζ. In the bottom panel the map of photon emission of energies above 100 GeV is presented with $\zeta = 48°$ marked.

upper limit is, therefore, the only constraint for the model, as far as the gamma-ray energy range is concerned. Pulsar parameters used in the simulations are: spin period $P = 5.757$ ms, dipolar magnetic field strength at the polar cap $B_{\rm pc} = 6.58 \cdot 10^8$ Gauss and distance $d =$ 140 pc. Calculations were performed for the geometrical configuration: $\alpha = 35°$, $\zeta = 40°$ (Manchester & Johnston, 1995). The Figure 3 presents the obtained results. For PSR J0437-

4715 we obtained gamma-ray energy spectra which differ from the single-particle spectra presented recently by Venter & De Jager (2005) for the same electric field model. Unlike in their case, our phase-averaged energy spectra below $\sim$ 1 GeV assume a power-law shape $F_E \propto E^p$ with the energy index $p \simeq 1/5$ for the case of $\alpha = 35°$, $\zeta = 40°$. Moreover, above $\sim$ 1 GeV the energy spectra changes the slope to $p \simeq -1$; high-energy cutoffs are reached at $\sim$ 10 GeV. In conclusion the pure SCLF-USEF model does not obey the limit inferred from EGRET observations. Similar conclusion was obtained by Venter & De Jager (2005) for their 'single-particle' spectra. Although the results are in conflict with the EGRET upper limit, the discrepancy is quite small (by a factor of 2) and may be elevated easily by introducing e.g. small-scale perturbations to the dipolar magnetic field.

5. PSR B1821-24

PSR B1821-24 belongs to the class of young (spin-down age of $3 \cdot 10^7$ yr) millisecond pulsars with non-thermal X-ray emission. Considering its spin-down luminosity $L_{\rm sd} = 2.2 \cdot 10^{36}$ erg/s makes it the most energetic MSP known. The pulsar parameters used in numerical calculations are: spin period $P = 3.05$ ms, magnetic field strength at the polar cap $B_{\rm pc} = 4.5 \cdot 10^9$ Gauss, and distance $d = 5.5$ kpc. For the geometrical configuration the inclination angle was chosen $\alpha = 50°$ (after Backer & Sallmen, 1997). The numerical results are presented in Figure 4. We found the electric field model by Muslimov & Harding (1997) applicable despite high energetics of this pulsar (i.e. high maximal potential drop $\Delta V_{\rm max}$) – the number of secondary e^+/e^- particles is not sufficient to effectively limit the accelerating region to the thin layer above the star surface. We also found the pulsar to produce enough high energy radiation ($E_{\rm ph} >$ 100 GeV) to be detectable by Cherenkov telescope H.E.S.S – which is not the case for the two other pulsars under consideration. Its detectability however depends on the uncertain geometry of the pulsar. If the line of sight crosses the narrow beam of such radiation the detection is possible. The extected photon flux is presented in Fig. 4. Its detection could be crucial to our understanding of pulsar high gamma emission mechanisms.

Acknowledgements. We enjoyed discussions with Jarek Dyks, Alice Harding, Okkie de Jager and Agnieszka Slowikowska. This work was supported by grant PBZ-KBN-054/P03/2001.

References

Backer, D. C. & Sallmen, S. T. 1997, AJ, 114, 1539
Baixeras, C. 2003, Nuclear Physics B Proceedings Supplements, 114, 247
Bulik, T., Rudak, B., & Dyks, J. 2000, MNRAS, 317, 97
Dyks, J. & Rudak, B. 2003, ApJ, 598, 1201
Fierro, J. M., Arzoumanian, Z., Bailes, M., et al. 1995, ApJ, 447, 807
Harding, A. K. & Muslimov, A. G. 1998, ApJ, 508, 328
Harding, A. K., Muslimov, A. G., & Zhang, B. 2002, ApJ, 576, 366
Harding, A. K., Usov, V. V., & Muslimov, A. G. 2005, ApJ, 622, 531
Konopelko, A. 2002, in Neutron Stars, Pulsars, and Supernova Remnants, 105–+
Konopelko, A. K. 1999, Astroparticle Physics, 11, 263
Kuiper, L., Hermsen, W., Verbunt, F., & Belloni, T. 1998, A&A, 336, 545
Kuiper, L., Hermsen, W., Verbunt, F., et al. 2000, A&A, 359, 615
Manchester, R. N. & Johnston, S. 1995, ApJ, 441, L65
Muslimov, A. & Harding, A. K. 1997, ApJ, 485, 735
Muslimov, A. G. & Harding, A. K. 2004, ApJ, 606, 1143
Rudak, B. & Dyks, J. 2002, in Proc. of the XXXVIIth Rencontres de Moriond, 119–124
Stairs, I. H., Thorsett, S. E., & Camilo, F. 1999, ApJS, 123, 627
Venter, C. & De Jager, O. C. 2005, ApJ, 619, L167